Journal of Advanced Scientific Research

Available online through https://sciensage.info

ISSN

0976-9595

Research Article

Characterization and Bactericidal Efficacy Studies of Silver Nanoparticles Synthesized from Leaf Extract of Medicinal Plant, *Ocimum basilicum*

MP Somashekarappa[1*], V Sowmya[2]

[1]Department of Studies in Chemistry, GFG College, Kadur, Chikkamagaluru, Affiliated to Kuvempu University, Karnataka State, India.

[2]Department of PG Studies in Chemistry, IDSG College, Chikkamagaluru, Affiliated to Kuvempu University, Karnataka State, India.

Corresponding author: mpsomashekar1@gmail.com

Received: 07-04-2024; Accepted: 28-04-2024; Published: 31-05-2024

https://doi.org/10.55218/JASR.2024150503

ABSTRACT

Silver nanoparticles (AgNPs) were synthesized using the leaf extract of *Ocimum basilicum*, a medicinal plant, as a reducing agent. Characterization of the particles was done by UV-visible extinction spectroscopy, scanning electron microscopy (SEM), transmission electron microscopy (TEM), and powder X-ray diffraction (PXRD) studies. The shapes of particles are spherical to quasi-spherical. Diffraction patterns from characteristic crystallographic planes observed in PXRD and concentric rings with bright intermittent dots observed in selected area x-ray diffraction (SAED) confirm that the silver in their nanoparticles is being crystallized into a face-centered cubic (FCC) structure. The average particle size worked out using PXRD data and the maximum of particle size distribution with respect to TEM analysis are 16 and 20 nm, respectively. Antibacterial efficacy of the synthesized AgNPs against the spreading of gram-negative bacteria, *Escherichia coli* and gram-positive bacteria, *Staphylococcuus aureus* were determined in terms of their minimum inhibitory concentration (MIC) in nutrient agar media, and the results were compared with that shown by ciprofloxacin, a reference substance. The MICs of the AgNP solutions synthesized from *O. basilicum* were 9.00×10^{-5} g/mL against the spread of *E. coli* and 1.125×10^{-4} g/mL against *S. aureus*. The antibacterial efficacy determined against *E. coli*, in the adopted procedure, of the AgNPs synthesized using the water extract of the leaf sample of *O. basilicum* is superior to that exhibited by ciprofloxacin.

Keywords: *Ocimum basilicum,* Silver nanoparticles, Antibacterial activity, Bactericidal efficacy, *Escherichia coli, Staphylococcus aureus.*

INTRODUCTION

Silver nanoparticles constitute a separate class of most studied metal nanoparticles[1] owing to their size-dependent surface plasmon resonance[2] and consequent remarkable electronic and optical properties.[3] The technical applications of the AgNPs encompass photocatalysis,[4] optical sensors,[5] nanosphere lithography,[6] optoelectronics,[7] solar energy conversion devices[8] and surface-enhanced Raman scattering (SERS) substrates[9] In addition, AgNPs exhibit antimicrobial effects[10] making them applicable in various biomedical fields.[11-13] The antimicrobial properties of the AgNPs have been manifested in making AgNP embedded polyurethane antibacterial water filters,[14] blotting paper-based point-to-use antibacterial water filters,[15-17] AgNP-embedded carbon-based antibacterial air filter[18] and AgNP tethered antibacterial textile fabrics.[19-22] AgNPs have also been proven to be applicable as carriers in drug delivery systems and the related literature precedents have been reviewed.[23]

Chemical reduction methods of synthesis of AgNPs involve using harsh chemical reducing agents, such as $NaBH_4$, $LiAlH_4$, $R_4N^+(Et_3BH^-)$ or hydrazine.[24] These methods yield unstable AgNP solutions contaminated with reaction by-products like borides, metal borates,[25] B_2H_6, $NaNO_3$, etc. In chemical reduction methods, stabilizing AgNPs solutions use stabilizing agents[26] such as certain polymers and cationic polynorbornenes.[27] This method makes the synthesis and stabilization of AgNPs expensive, harmful and multistep one's. Therefore, it is important to identify the greener, cheaper and eco-friendly methods and resources for the synthesis of stable AgNP solutions with minimum or no reaction by-products, which contaminate the system. Using extracts of plants, bacteria, fungi and biopolymers for the synthesis of AgNPs is a greener, cheaper and more eco-friendly method in recent years.[28-30] In addition to the method of synthesis being greener, cheaper and eco-friendly, the AgNPs synthesized using plant extracts are found to be more sensitive for biosensing of fungicides and photocatalytic activity[31] and have wider pharmacological applications in the treatment of cancer, malaria, microbial and cardiovascular diseases.[32]

We found therefore, screening medicinal plants for their phytonutrients to be useful as mild reductants and stabilizing agents for the synthesis of AgNPs, interesting and important as well. It was estimated by WHO in 1999 that "in many developing countries, a large proportion of the population relies heavily on traditional practitioners and medicinal plants to meet primary health care needs",[33] and "there has been a tremendous increase in the use of herbal medicine" through the year 2009[34] Therefore it indicates that

it is important to depend on natural plant resources for doing simple reduction chemistry to arrive at sensitive materials for antimicrobial and pharmacological applications.

The results presented and discussed in this paper are those obtained from an important medicinal plant, *Ocimum basilicum*, used in India. *O. basilicum* is a very important plant containing essential oils, polyphenols, phenolics, flavonoids and phenolic acids, whose pharmacological uses include anti-cancer activity, radioprotective activity, antimicrobial activity, anti-inflammatory effects, immunomodulatory activity, anti-stress activity, anti-diabetic activity, antipyretic activity, anti-arthritic activity and anti-oxidant activity.[35] Reports on biomedical activities of the extracts of *O. basilicum* have been reviewed.[36]

This paper describes the synthesis of stable AgNPs using the water extract of the leaf samples of *O. basilicum*, *the* characterization of the AgNPs through Uv-visible absorption spectroscopy, PXRD, SEM and TEM analyses, and the study of their bactericidal effects against *E. coli* and *S. aureus* bacteria.

MATERIALS AND METHODS

Materials

The chemicals are from Merck, and from S. D. Fine chemicals. The nutrient agar media is from Himedia. Distilled water was used wherever required. The bacteria selected for the study were *E. coli* and *S. aureus*. A laboratory centrifuge, R-8C from Remi was used for the isolation of particles for SEM and powder XRD analyses. Systronics UV-visible spectrophotometer 119 was used for recording the UV-visible extinction spectra in the wavelength range of 300 to 700 nm. Powder XRD patterns were recorded on a Rigacu Smartlab X-ray diffractometer and the SEM and EDS were recorded on an Ultra 55 scanning electron microscope from GEMINI technology. TEM imaging on the drop casted samples was done on Titan Themis 300kV from FEI.

Methods

Extraction

Freshly collected leaves of the plants were sliced and crushed into a paste with a small amount of warm distilled water using a mortar and pestle. The paste was transferred into a 250 mL beaker, suspended in 100 mL water, stirred on a magnetic stirrer for about 30 minutes at 45 to 50°C temperature, cooled to lab temperature and filtered through a pre-weighed piece of qualitative filter paper. The difference in weight method calculated the weight of the contents transferred to the extract. Qualitative phytochemical analysis of the extract was done following a routine method.[37]

Synthesis of silver nanoparticles

About 50 mL of the fresh extract containing approximately 0.04 ± 0.005 g/mL of extracted substances was taken in a round-bottomed flask fitted with a pressure-equalizing dropping funnel. It was heated to 60°C while stirring and 20 mL of 0.002 M $AgNO_3$ solution was added dropwise. Temperature was maintained at 60 ± 5°C during the addition of $AgNO_3$ solution and for a further 1 hour. Contents were cooled to lab temperature. The AgNP solution so obtained was centrifuged in order to isolate the material for powder XRD and SEM analyses. The solid was then dried in a vacuum over anhydrous phosphorous pentoxide and powdered.

Antibacterial activity studies

A known volume of the AgNP solution was evaporated on a pre-weighed watch glass, dried and weighed to determine the amount of AgNP material in its solution. A suspension of 28 grams of nutrient agar in 1000 mL of distilled water was boiled and autoclaved. 20 mL aliquots of the nutrient agar media were contaminated with various increased concentrations of AgNP solutions and transferred into sterilized Petri dishes placed in the sterilized laminar airflow chamber. When the media hardened, the surface of the media was applied with stains of selected bacteria using cotton swabs. The growth or spread of bacteria was followed for a period of 12 to 15 hours. The standard reference for analysis of the data was the results of the same experiments using ciprofloxacin conducted at the same condition.

RESULTS AND DISCUSSION

Phytochemical Analysis

A qualitative phytochemical analysis using routine procedures[37] was applied to the water extract with a phytonutrient concentration of ~25 $\times 10^{-3}$ g/mL of the leaf sample of *O. basilicum*. The results of phytochemical screening are presented in Table 1. It is interesting to note that the extract of the plant reveals the presence of carbohydrates and glycosides, proteins and amino acids, and phenolic acids and flavonoids. The results of our analyses are consistent with those reported by earlier researchers.[35]

The size, shape, concentration, surface charge, colloidal state and agglomeration are very important physicochemical parameters required for AgNPs to be useful for biomedical applications.[28,38] Compared to the physical and chemical methods, biological methods are highly diverse and eco-friendly in nature because of the natural origin of the reduction, dispersion and stabilizing medium. Secondary metabolites or the phytonutrients in the plant extract, such as phenolic compounds, flavones and triterpenoids, render the extract with free radical scavenging ability,[39-41] and hence make the extract comfortably reducing in nature.

Synthesis

The procedure adopted for the synthesis of AgNPs using the selected plant does not involve any reducing agent and stabilizing molecules. The procedure followed is highly reproducible. Various phenolic compounds and flavonoids present in the extract reduce the Ag^+ in the $AgNO_3$ into atomic silver,[30,39-41] which further coalesce to form nanosized AgNPs. As soon as particles are formed, the oxidized secondary metabolites of the extract, after reduction and other bioactive and functional molecules not involved in reduction, form a monomolecular layer on the particles.[26,32] The stability of the dispersion of the particles can be attributed to the mutual repulsion between individual particles as all of them possess the same charge, being coated by a monomolecular layer of the same kind of phytonutrient molecules.

Characterization

Fig. 1(b) shows the UV-visible absorption spectrum of the AgNP solution synthesized using leaf extract of *O. basilicum*.

Table 1: The results of phytochemical analysis of the leaf extracts of *O. basilicum*

Phytonutrient	*Test*	*Inference*
Alkaloids	Mayers Test	–
	Wagners test	–
	Hagers test	–
Carbohydrates and glycosides	Molish test	+
	Fehling's test	+
	Benedicts test	–
	Barfoed's test	–
Saponins	Foam test	–
Proteins and amino acids	Millons's test	–
	Biuret's test	–
	Ninhydrin test	+
Phytosteriods	Libeirman – Burchards test	–
Oils and fats	Spot test	–
	Saponification test	–
Phenolic compounds and flavonides	Ferric chloride test	+
	Lead acetate test	+
	Alkaline test	+
	Gelatin test	–
Gums and mucilages		–

A characteristic surface plasmon resonance absorption band in the UV-visible region of electromagnetic radiation[42,43] is used for the initial identification of AgNPs. The appearance of a reddish brown color upon the reaction of pale green plant extract with $AgNO_3$ solution is indicative of the formation of AgNPs. However, it can be confirmed by recording the UV-visible spectrum between 300 and 700 nm.[44,45] Recording an absorption spectrum in the same region for dilute leaf extract of *O. basilicum* does not show any absorption peak but only a baseline (Fig.1: (a)). However, a relatively wider peak with a maximum of 433 nm is indicative of the formation of AgNPs in the solution (Fig.1: (b)). The bigger full width at half maximum (FWHM) of the absorption peak could be ascribed to the overlapping of several sharp absorption bands, qualitatively representing a wider particle size distribution.

UV-visible absorption spectral data of the AgNPs synthesized using both the selected plants are consistent with that of AgNPs synthesized using hydrazine hydrate and sodium citrate as reducing agents.[46] Repeated recording of the spectrum between 300 and 700 nm for the AgNP solution with regular intervals for a period of 12 weeks shows no decrease in intensity of the characteristic absorption peaks. This indicates a good stability of the of the particles in the dispersion medium.

Two separate sets of experiments have been conducted to understand the dependence of concentrations of phytonutrients in extract and the concentration of $AgNO_3$ on the particle size of the AgNPs obtained and the data are presented in Figs. 2 and 3, respectively. In the present adopted method, when a solution $AgNO_3$ is maintained constant at 6.0×10^{-5} M and when the concentration of phytonutrients increases from 3.90×10^{-5} to 19.50×10^{-5} g/mL, the λ_{max} in the respective UV-visible spectra decreases from 445 to 433 nm. It has been established that the particle size of AgNPs could be estimated using UV-visible light spectroscopy.[44] The decrease in the λ_{max} for the AgNP solutions is attributed to the decrease in the particle size[44] as the phytonutrient concentration increases. The decrease in particle size with respect to the increase in phytonutrient concentration is understood to be as follows. As the concentration of the phytonutrients increases, with the limited concentration of 6.0×10^{-5} M $AgNO_3$, the rate of reduction increases and hence, the particles are formed at a relatively higher speed. As soon as the Ag^+ in the $AgNO_3$ reduces to Ag^0 and coalesces into particles, they get capped by the reduction products of, as well as unused phytonutrient molecules present in the extract, at the reaction temperature. Preferential rapid capping of the particles restricts the growth of particles into smaller-sized ones. Thus, an increase in phytonutrient concentration

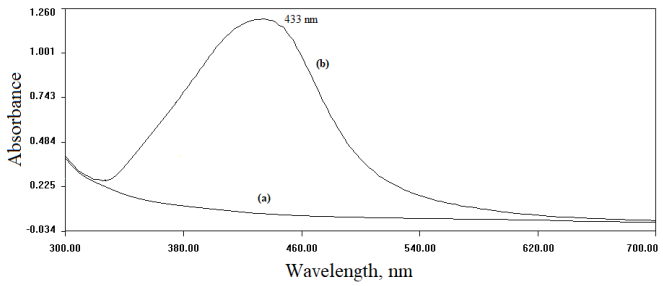

Fig. 1: Uv-visible absorption spectrum of (a) extract of *O. basilicum* with phytonutrient concentration of 19.50×10^{-5} g/mL, and (b) AgNP solution prepared using leaf extract of *O. basilicum*

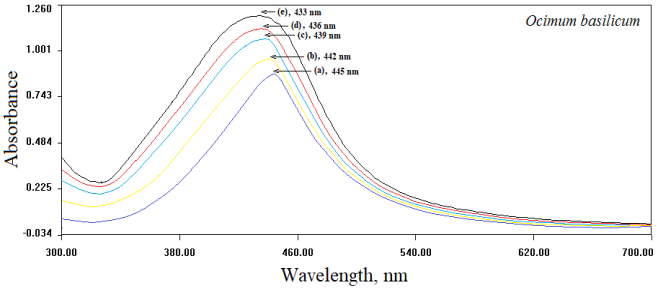

Fig. 2: UV-visible absorption spectra of AgNP solutions synthesized by reacting 6.0×10^{-5} M $AgNO_3$ solution with the water extract of *O. basilicum*, containing (a) 3.90×10^{-5} g/mL, (b) 7.80×10^{-5} g/mL, (c) 11.7×10^{-5} g/mL, (d) 15.6×10^{-5} g/mL, (e) 19.50×10^{-5} g/mL, of phytonutrients

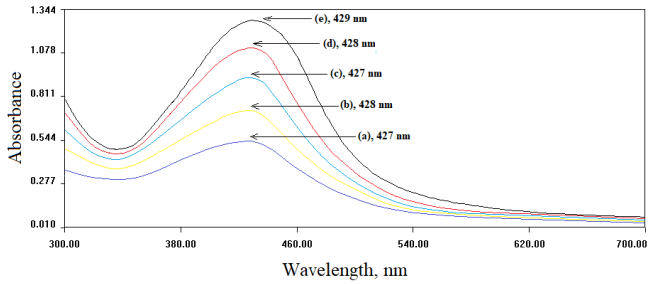

Fig. 3: Uv visible absorption spectra of AgNP solutions prepared by reacting water extract of *O. basilicum* having phytonutrient concentration of 2.0×10^{-4} g /mL with (a) 6.2×10^{-5} M, (b) 1.24×10^{-4} M, (c) 1.86×10^{-4} M, (d) 2.48×10^{-4} M, (e) 3.1×10^{-4} M $AgNO_3$ solution

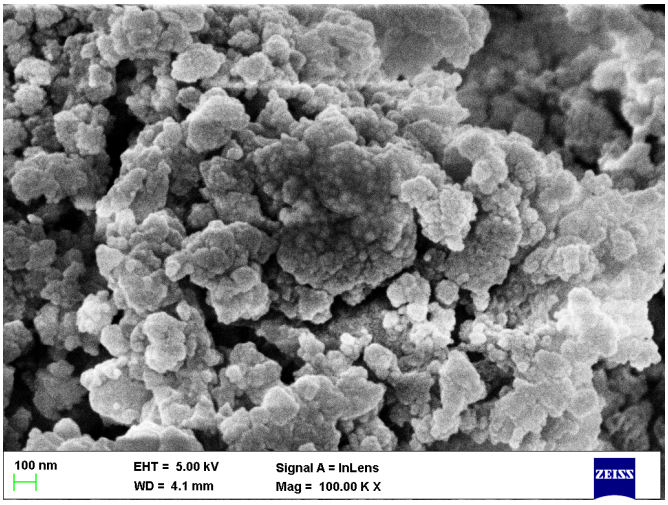

Fig. 4: Scanning electron micrograph of AgNPs synthesized from the aqueous leaf extract of *O. basilicum*

increases the rate of reduction followed by instantaneous capping of the AgNPs formed by phytonutrient molecules, resulting in a decrease in λ_{max} in their uv-visible absorption spectra (from Fig. 2(a)-(e)). A slight increase in the intensity of UV-visible absorption peaks with respect to the consequent increase in phytonutrient concentration (Fig. 3(a)-(e)) could be accounted for an increase in yield of AgNPs as a result of respective consequent decrease in particle size.

In another series of individual experiments, the concentration of $AgNO_3$ solution added was increased with a fixed, relatively high (2.0×10^{-4} g /mL) concentration of phytonutrients in order to check the dependence of particle size upon $AgNO_3$ concentration. The results obtained are consolidated in Fig. 3. No considerably bigger and regular trend in the variation of λ_{max}, in the uv-visible extinction spectra have been noticed when the concentration of $AgNO_3$ increased from 6.2×10^{-5} M (Fig. 4(a)) to 3.1×10^{-4} M (Fig. 4(e)). This observation indicates that an increase in the concentration of $AgNO_3$ at a fixed excess concentration of phytonutrients do not affect the particle size of the AgNPs. This could be understood as follows. The particle size of the completely capped AgNPs depends on the rate of reduction and the consequent formation of a molecular layer of phytochemical molecules or capping upon the bare particles. The rate of reduction depends solely on the concentration of reduction medium of the extract and not on the concentration of the source of metallic silver that is concentration of $AgNO_3$ available.

Fig. 4 shows the SEM images of the AgNPs synthesized from the leaf extract of *O. basilicum* and isolated by centrifugation at 4000 rpm.

SEM image of the powder samples isolated from the AgNP solutions (Fig. 5) reveals that the spherical particles coalesce to bigger spherical micron-sized aggregates. Aggregation must have taken place as the organic monolayer-covered particles are pressed upon each other during centrifugation in order to isolate the material.

The elements present in the isolated AgNP material synthesized form *O. basilicum* are profiled using EDS studies and the data are presented in Fig. 5.

Analysis of the EDS data shows 47% by weight of silver followed by 18% carbon, 6% nitrogen and 29% oxygen (insets in Fig. 5(b). The presence of carbon, nitrogen and oxygen in the EDS data is attributable to the formation of a monomolecular layer of the phytonutrient molecules around the particles in order to stabilize them.

TEM images recorded upon drop casted samples of the AgNPs synthesized from *O. basilicum* is shown in Fig. 6.

The shapes of the particles are spherical to quasi-spherical and our observation is in conformity with earlier reports. The shapes of AgNPs synthesized from the plant extract of *Terminalia bellirica,*[47] and those obtained by extracellular synthesis using fungus *Aspergillus niger* are spherical.[48] In contrast, the particles synthesized using an extract of apiin as a reducing agent are quasi-spherical in shape.[49] The particle size distribution of the AgNPs obtained in the present study was worked out and presented as histogram fit as inset in Fig. 6. The size distribution histogram shows that the maximum of particle size distribution curve passess through 20 nm (inset in Fig. 6). The relatively bigger aggregates of the AgNP material appeared during SEM analyses, as shown in Fig. 4 must have been the result of aggregation of the nanosized particles in to bigger lumps as the particles covered with a monolayer of phytonutrient molecules pressed upon each other during centrifugation and consequent drying process in vacuum. This aggregation could be further looked closely into as a phenomenon in which the organic phytonutrient molecular layer anchored on the adjacent silver particles undergoes interdigitation under the influence of centrifugal force. This results in the aggregation of individual particles. A high-resolution TEM image of a single 27 nm particle is presented in Fig. 7(a).

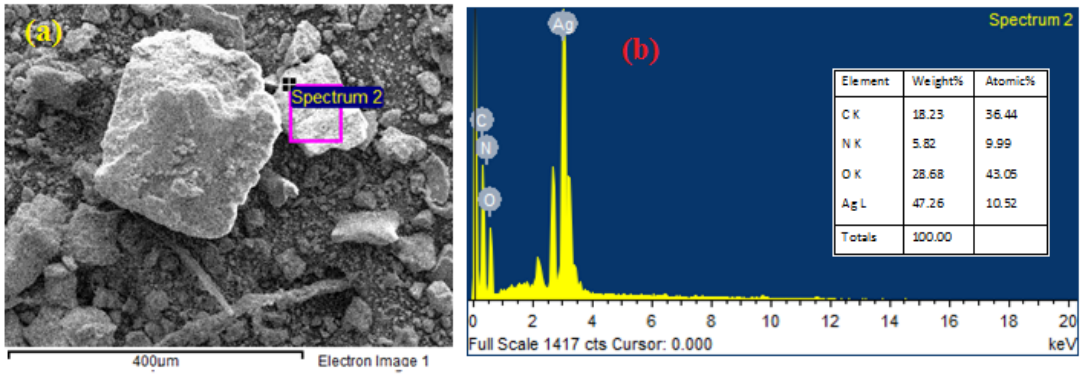

Fig. 5: (a) Micron sized material lumps upon which the point EDS was recorded and (b) the EDS spectrum of the silver nanoparticles synthesized using the leaf extract of *O. basilicum*. Inset in (b): Table showing the elemental percentage of silver, carbon, nitrogen and oxygen in the material

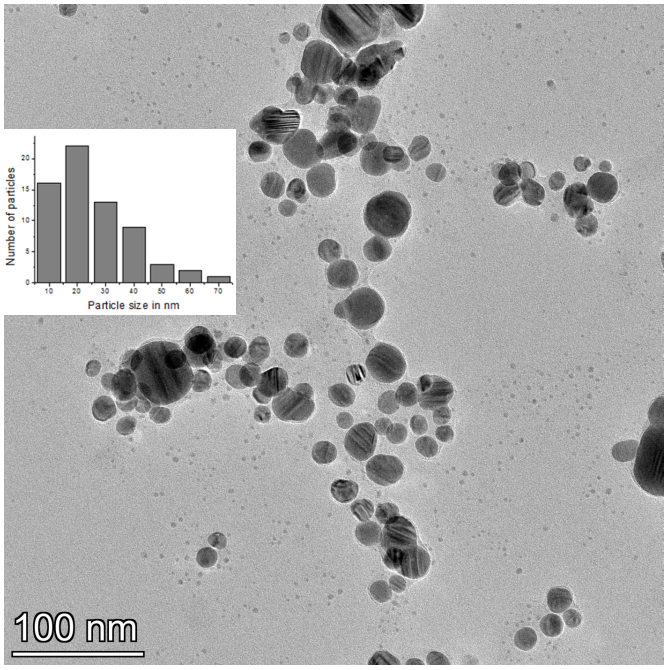

Fig. 6: Transmission electron micrographic image of the AgNPs synthesized from the extracts of O. basilicum. Inset: Histogram showing the particle size distribution worked out upon TEM image

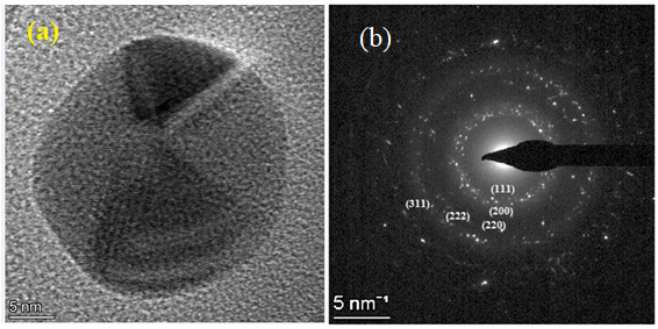

Fig.7: (a) High-resolution TEM image of the single 27 nm sized silver nanoparticle synthesized from the leaf extract of *O. basilicum*. (b) SAED pattern on the drop casted layer of AgNP solution

Fig. 7(b) shows the selected area electron diffraction (SAED) pattern recorded on a drop casted thin layer of AgNPs solution synthesized using water extract of *O. basilicum*, and the pattern exhibits concentric rings embedded with bright intermittent spots. The consecutively increasing radii of these concentric rings represent electron diffraction from (111), (200), (220), (222) and (311) planes of face-centered cubic (FCC) structure of crystalline metallic silver in AgNPs. This confirms that the phytonutrient molecules present in the extract of the selected plant reduce the silver nitrate molecules into atomic silver and the resulting metallic silver crystalizes into an FCC structure in their nanoparticles.[46] TEM analysis in this work is in good agreement with that obtained for the AgNPs synthesized both by chemical reduction method and by using extract of *Hibiscus rosasinensis*.[50]

The powder XRD patterns were recorded on the dried samples of the AgNP material synthesized using an extract of Ocimum bailicum and isolated by centrifugation and presented in Fig. 8.

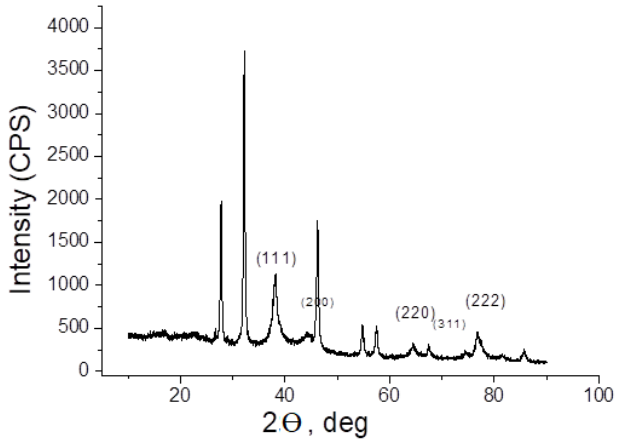

Fig. 8: Powder XRD pattern of AgNPs synthesized from the leaf extract of *O. basilicum*

The characteristic positions of the peaks corresponding to the crystallographic planes (111), (200), (220), (222) and (311) in the XRD pattern indicate the presence of silver being formed by the reduction of silver nitrate when added and stirred in the dilute solution of phytonutrient molecules. Further, it is understood that the reduced metallic silver crystalizes to face-centered cubic (FCC) structure. The wider full width at half maximum (FWHM) of the peaks in the presented PXRD pattern indicates that the material is of nanocrystalline form. The average particle size is calculated using Debye – Scherrer's formula, where $D = 0.94\ \lambda/\beta \cos\theta$, where D is the average crystalline size, λ is the wavelength of X-ray = 0.154056 nm, β is FWHM and θ is the angle of diffraction, with respect to (111) crystallographic plane and is 16 nm.

The peak positions corresponding to various crystallographic planes in the PXRD patterns obtained for the AgNPs, in the present study are comparable and in good agreement with PXRD patterns recorded for AgNPs synthesized using aqueous extract of *Ocimum Sanctum and* quercetin (a flavonoid from the same plant) [38], root hair extract of *Phoenix dactylifera,*[51] *extracts of garlic, green tea and turmeric,*[52] extract of *Sida cordifolia*.[53] *The other sharp peaks in the PXRD patterns* may be attributed to the possible crystallization of other phytonutrient molecules, which are not involved either in the reduction of $AgNO_3$ or capping of the particles on their surface or particle aggregates.

Antimicribial Activity Studies

The use of silver and a few other metals such as copper, iron, lead, tin, and alloys like brass and bronze for therapeutic purposes have been very much known in ancient Indian ayurvedic medicinal practice for thousands of years,[54] wherein the traditional form of silver used in ayurvedic medicine has been understood to work as drug bio-enhancer with medicine or pharmaceuticals.[55] Thus, silver nanoparticles are very much known to possess characteristic antimicrobial activities.[56] Precedents pertaining to the antimicrobial activity studies upon silver nanoparticles synthesized by all possible methods have been reviewed elaborately.[57,58] In the present work, experiments were conducted to make a relative assessment of the bactericidal ability of AgNPs synthesized using leaf extract of *O. basilicum,* against two bacteria *E. coli* and *S. aureus*. Bactericidal efficacy was obtained in terms of minimum inhibitory concentration (MIC) of

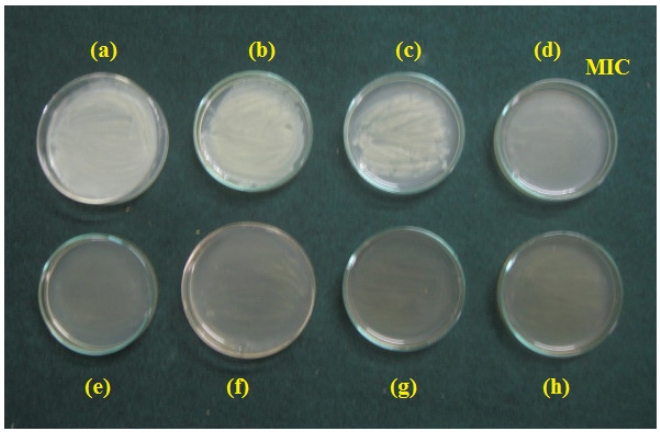

Fig. 9: Growth of the *E. coli* bacteria in 20 mL nutrient agar media contaminated with (a) 0.00 g/mL. (b) 4.50×10^{-5} g/mL, (c) 6.75×10^{-5} g/mL, (d) 9.00×10^{-5} g/mL (e) 1.125×10^{-4} g/mL, (f) 1.35×10^{-4} g/mL (g) 1.575×10^{-4} g/mL, (h) 1.80×10^{-4} g/mL of silver nanoparticles prepared from extract of *O. basilicum*

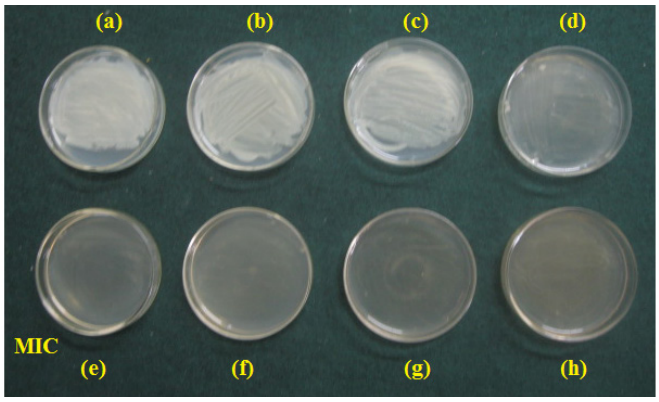

Fig. 10: Growth of the *Staphylococcus aureus* bacteria in 20 mL nutrient agar media contaminated with (a) 0.00 g/mL. (b) 4.50×10^{-5} g/mL, (c) 6.75×10^{-5} g/mL, (d) 9.00×10^{-5} g/mL (e) 1.125×10^{-4} g/mL, (f) 1.35×10^{-4} g/mL (g) 1.575×10^{-4} g/mL, (h) 1.80×10^{-4} g/mL of silver nanoparticles prepared from extract of *O. basilicum*

AgNPs in their solid solution in nutrient agar media. The determined MICs of the AgNPs against *E. coli* and *S. aureus* are presented in Figs 9 and 10, respectively.

Figs 9 and 10 reveal that an increase in the concentration of AgNPs in the solidified nutrient agar media results in a lowering of growth of both the bacteria selected for the study. The lowest possible concentration of AgNPs at and above which the bacterial growth is completely diminished, is understood as MIC of the AgNPs. The determined MIC of the AgNPs is compared with that determined for a standard reference substance, ciprofloxacin, in parallel experiments. The MICs determined for AgNPs synthesized using the extract of *O. basilicum* are highly reproducible and work out to be 9.00×10^{-5} and 1.125×10^{-4} g/mL, respectively, against *E. coli* and *Staphylococcus aureus*. However, the experimentally determined MICs of the ciprofloxacin are 20×10^{-5} g/mL against *E. coli* and 24×10^{-5} g/mL against *S. aureus* bacteria in the same experimental conditions. Thus, the antibacterial efficacy against *E. coli*, determined in the adopted procedure, of the AgNPs synthesized using the water extract of the leaf sample of *O. basilicum* is superior to that exhibited by ciprofloxacin.

CONCLUSION

Systematic phytochemical analyses of the water extract of the title plant O. basilicum reveal the presence of carbohydrates and glycosides, proteins and amino acids, and phenolic acids and flavonoids, which reduce silver nitrate into metallic silver in the adopted experimental condition. The atomic silver thus obtained crystallizes into a face-centered cubic structure in the form of nanosized particles whose surfaces are instantly capped through a mechanism of formation of a monomolecular layer of phytonutrient molecules, which are either oxidized by reducing silver nitrate or unreacted ones. The AgNP solutions so obtained are highly stable and the stability could be ascribed to some degree of repulsion between the individual particles possessing the same surface charge, because of the same molecular characteristics of the of the monomolecular layer around them. Particles are spherical to quasi-spherical shaped as visualized by TEM analysis and the particle size distribution passes across 20 nm. The particle size calculated with respect to the (111) crystallographic plane in the PXRD pattern is 16 nm. The crystallographic planes (111), (200), (220), (222) and (311) identified in the PXRD pattern agree well with the concentric rings observed in the SAED pattern and are consistent with the FCC structure of the silver in their nanoparticles. *The MICs of AgNPs synthesized using the water extract of O. basilicum are* 9.00×10^{-5} g/mL and 1.125×10^{-4} g/mL, *respectively, against the growth of E. coli* and *S. aureus*. Thus, the antibacterial efficacy determined in the adopted procedure of the AgNPs synthesized using the water extract of the leaf sample of *O. basilicum* is superior to that exhibited by ciprofloxacin.

ACKNOWLEDGEMENTS

The authors thank VGST for awarding a K-FIST level-1 grant, which was used to establish a basic laboratory facility. The author also thanks the Micro and Nano characterization facility, Center for Nanoscience and Engineering, IISc., Bangalore for extending characterization support under INUP program. The authors also thank Dr. B. Thippeswamy, Department of Microbiology, Kuvempu University, for providing bacteria.

This research did not receive any specific grant from funding agencies in the public, commercial, or not-for-profit sectors.

CONFLICT OF INTEREST

The authors declare that they have no conflicts of interest.

REFERENCES

1. Beyene HD, Werkneh AA, Bezabh HK, Ambaye TG, *Sustain Mater Technol*, 2017; **13:**18-23.
2. Stark WJ, Stoessel PR, Wohlleben W, Haffner A, *Chem Soc Rev*, 2015; **44**:5793-5905.
3. Amendola V, Bakr OM, Stellacci F, *Plasmonics*, 2010; **5:**85-97.
4. Awazu K, Fujimaki M, Rockstuhl C, Tominaga J, Murakami H, Ohki Y, et al. *J Am Chem Soc*, 2008; **130(5)**:1676-1680.
5. McFarland AD, Van Duyene RP, *Nano Lett*, 2003; **3**:1057-1062.
6. Jensen TR, Malinsky MD, Haynes CL, Van. Duyne RP, *J Phys Chem B*, 2000; **104**:10549–10556.
7. Ko S-J, Choi H, Lee W, Kim T, Lee BR, Jung J-W, et al. *Energ Environ Sci,* 2013; *6*:1949-1955.
8. Morfa AJ, Rowlen KL, *Appl Phys Lett*, 2008; **92**:013504.

9. Li W, Guo Y, Zhang P, *J Phys Chem C*, 2010; **114**:6413–6417.
10. Rai M, Yadav A, Gade A, *Biotechnol Adv*, 2009; **27**:76–83.
11. Wong KKY, Liu X, *Med Chem Commun*, 2010; **1**:125 131.
12. Prabhu S, Poulose EK, *Int Nano Lett*, 2012; **2**:32.
13. Burdusel AC, Gherasim O, Grumezescu AM, Mogoanta L, Ficai A, Andronescu E. *Nanomaterials*, 2018; **8(9)**:681.
14. Jain P, Pradeep T, *Biotechnol Bioeng*, 2005; **90**:59.
15. Dankovick TA, Gray DG, *Environ Sci Technol*, 2011; **45**:1992–1998.
16. Praveena SM, Karuppaiah K, Than LTL, *Cellulose*, 2018; **25**:2647–2658.
17. Yoon KY, Byeon JH, Park CW, Hwang J, *Environ Sci Technol*, 2008; **42**:1251–1255.
18. Ravindra S, Mohan YM, Reddy NN, Raju KM, *Colloids Surf A: Physicochem Eng Asp*, 2010; **367**:31-40.
19. Song J, Kang H, Lee C, Hwang SH, Jang J, *ACS Appl Mater Interfaces*, 2012; **4**: 460-465.
20. Wu M, Ma B, Pan T, Chen S, Sun J, *Adv Functional Mater*, 2016; **26(4)**:569-576.
21. Zhang S, Tang Y, Vlahovic B, *Nanoscale Res Lett*, 2016; **11**: 80.
22. Shaki Devi R, Girigoswami A, Siddarth M, Girigoswami K, *Appl Biochem Biotechnol*, 2022; **194**:4186-4219.
23. Chandrakala V, Aruna V, Angajala G, *Emergent Mater*, 2022; **5:**1593-1615.
24. Schmid G, Chi LF, *Adv Mater*, 1998; **10**:515-526.
25. Glavee GN, Klabunde KJ, Sorensen CM, Hadjapanayis, *Langmuir*, 1992; **8**:771-773.
26. Garcia-Barrasa J, López-de-Luzuriaga JM, Monge M, *Cent Eur J Chem*, 2011; **9**:7-19.
27. Baruah B, Gabriel GJ, Akbashey MJ, Booher ME, *Langmuir*, 2013; **29**:4225- 4234.
28. Sharma VK, Yngard RA, Lin Y, *Adv Colloid and Interface Sci*, 2008; **145**:83–96.
29. Mittal AK, Chisti Y, Banerjee UC, *Biotechnol Adv*, 2013; **31**:346–356.
30. Rajeshkumar S, Bharath LV, *Chem – Biol Interactions*, 2017; **273**:219 –227.
31. Tarannum M, Divya, Gautam YK, *RSC Adv*, 2019; **9**:34926–34948.
32. Alex KV, Pavai PT, Rugmini R, Shiva Prasad M, Kamakshi K, Chandrashekar K, *ACS Omega*, 2020; **5(22)**:13123-13129.
33. Xulu JH, Ndongwe T, Ezealisiji KM, Tembu VJ, Mncwangi NP, Witika BA, et al. *Pharmaceutics*, 2022; **14:**2437.
34. Deng M, Yun X, Ren S, Quing Z, Luo F, *Molecule*s, 2022; **27(9):**2826.
35. Yob NJ, Jofrry SM, Meor Mohd Affridi MMR, The LK, Salleh MZ, Zakira ZA, *Evid Based Complement Alternat Med*, *2011; Article ID 543216.*
36. *Singh YP, Girisa S, Banik K, Ghosh S, Swathi P, Deka M, et al. J Funct Foods, 2019;* **53:***248-258.*
37. Raaman N, *Phytochemical Techniques*, New India, Publishing Agency, New Delhi, 2006.
38. Jain S, Mehata, MS, *Scientific Reports*, 2017; **7:** Article 15867.
39. Mandal D, Kumar Dash S, Das B, Chattopadhyay S, Ghosh T, Das D, et al. *Biomed. Pharmacother*, 2016; **83**:548-558.
40. Priya RS, Geetha D, Ramesh PS, *Ecotoxicol Environ* Saf, 2016; **134**:308–318.
41. Gopinath K, Kumaraguru S, Bhakyaraj K, Mohan S, Venkatesh KS, Esakkirajan M, et al. *Microb Pathog*, 2016; **101**:1-11.
42. Taleb A, Petit C, Pileni MP, *J Phys Chem B*, 1998; **102**:2214-2220.
43. Nogin ov MA, Zhu G, Bahoura M, Adegoke J, Small CE, Ritzo BA, et al. *Opt Lett*, 2006; **31(20)**:3022-3024.
44. Paramelle D, Sadovoy A, Gorelik S, Free P, Hobley J, Fernig DH, *Analyst***, 2014; 139(19):**4855-4861.
45. Desai R, Mankad V, Gupta SK, Jha PK, *Nanosci Nanotechnol Lett*, 2012; **4**:30-34.
46. Guzman MG, Dille J, Godet S, *Int J Chem Biomol Eng*, 2009; **2**:104–111.
47. Anand KKH, Mandal BK, *Spectrochim Acta A Mol Biomol Spectrosc*, 2015; **135:**639-645.
48. Gade AK, Bonde P, Ingle AP, Marcato PD, Duran N, Rai MK, *J Biobased Mater Bioenergy*, 2008; **2(3)**:243-247.
49. Kasturi J, Veerapandian S, Rajendran N, *Colloids and Surfaces B: Biointerfaces*, 2009; **68(1):**55-60.
50. Philip D, *Physica E: Low Dimens Sys. Nanostruct*, 2010; **42:**1417–1424.
51. Oves M, Aslam M, Rauf MA, Qayyum S, Qari HA, Khan MS, et al. *Mater Sci Eng C*, 2018; **89:**429-443.
52. Selvan DA, Mahendran D, Senthil Kumar R, Rahiman AK, *J Photochem Photobiol B: Biol*, 2018; **180:**243 – 252.
53. Pallela PNVK, Ummey S, Ruddaraju LK, Pammi SVN, Yoon S-G, *Microb Pathog*, 2018; **124:**63-69.
54. Galib, Mayur Barve, Mayur Mashru, Chandrashekhar Jagtap, Patgiri BJ, Prajapathi PK, *J-AIM*, 2011; **2(2):**55-63.
55. Sirisha Mukkavalli, Vijay Chalivendra, Bal Ram Singh, *OpenNano*, 2017; **2:**19-27.
56. Xiu ZM, Zhang QB, Puppala HL, Colvin VL, Alvarez PJJ, *Nano Lett*, 2012; **12(8):**4271–4275.
57. Le Ouay B, Stellacci F, *Nanotoday*, 2015; **10(3):**339 –354.
58. Roy A, Bulut O, Some S, Mandal AK, Yilmaz MD, *RSC Adv*, 2019; **9:**2673–2702.

HOW TO CITE THIS ARTICLE: Somashekarappa MP, Sowmya V. Characterization and Bactericidal Efficacy Studies of Silver Nanoparticles Synthesized from Leaf Extract of Medicinal Plant, *Ocimum basilicum*. *J Adv Sci Res*. 2024;15(5): 12-18 **DOI:** 10.55218/JASR.2024150503